

Physical Layer Secure Communications Based on Collaborative Beamforming for UAV Networks: A Multi-objective Optimization Approach

Jiahui Li[†], Hui Kang[†], Geng Sun^{†*}, Shuang Liang[†], Yanheng Liu[†], Ying Zhang[‡]

[†]College of Computer Science and Technology, Jilin University, Changchun 130012, China

[‡]School of Electrical and Computer Engineering, Georgia Institute of Technology, Atlanta 30332, USA

{lijiahui0803, liangshuang8587}@foxmail.com, {kanghui, sungeng, yhliu}@jlu.edu.cn, yzhang@gatech.edu

*Corresponding author: Geng Sun

Abstract—Unmanned aerial vehicle (UAV) communications and networks are promising technologies in the forthcoming fifth-generation wireless communications. However, they have the challenges for realizing secure communications. In this paper, we consider to construct a virtual antenna array consists UAV elements and use collaborative beamforming (CB) to achieve the UAV secure communications with different base stations (BSs), subject to the known and unknown eavesdroppers on the ground. To achieve a better secure performance, the UAV elements can fly to optimal positions with optimal excitation current weights for performing CB transmissions. However, this leads to extra motion energy consumptions. We formulate a secure communication multi-objective optimization problem (MOP) of UAV networks to simultaneously improve the total secrecy rates, total maximum sidelobe levels (SLLs) and total motion energy consumptions of UAVs by jointly optimizing the positions and excitation current weights of UAVs, and the order of communicating with different BSs. Due to the complexity and NP-hardness of the formulated MOP, we propose an improved multi-objective dragonfly algorithm with chaotic solution initialization and hybrid solution update operators (IMODACH) to solve the problem. Simulation results verify that the proposed IMODACH can effectively solve the formulated MOP and it has better performance than some other benchmark approaches.

Index Terms—UAV communications, collaborative beamforming, physical layer security, multi-objective optimization problem, evolutionary computation.

I. INTRODUCTION

Unmanned aerial vehicles (UAVs) that also commonly known as drones, are widely used in many domains such as the military, civilian and commercial applications, due to their advantages of high mobility, low cost, wide-coverage and simple deployment [1] [2]. In recent years, wireless communications and networks enabled by using UAVs have attracted increasing interest [3]. For example, UAVs can assist the wireless communications, e.g., the forthcoming fifth-generation (5G) wireless networks [4], which means that they are used as the flight base stations (BSs) or they can be flexibly deployed on demand to serve the ground users [5]. Moreover, UAVs can be also regarded as the new sky users in the classical cellular networks, e.g., the users on the ground can control and communicate with the UAVs remotely through the 5G networks [6].

Despite the promising applications, UAV communication and network systems will face many unprecedented challenges such as the limited on-board energy, restricted transmit power and long-range communications, etc [7] [8]. In particular, the security and privacy of the UAV communications are of utmost concern due to the broadcast nature of the wireless channels and line-of-sight (LoS) links between the UAVs and ground receivers, especially in outdoor scenarios [9] [10]. The upper-layer encryption is a common secure scheme for achieving confidential communications in wireless communications. However, this method may have challenges for UAVs because it needs high computation abilities, which is difficult for a UAV with limited hardware resources.

As an effective information secure scheme, the physical layer security (PLS) exploits the channel characteristics to hide information from the unauthorized receivers and thus it does not need complex encryption and decryption operations, which may be more suitable for UAV communications. However, using PLS in UAV-enabled wireless networks still has two major challenges. *First*, the achievable transmission rate is very limited if the distance between the UAV transmitter and legitimate receiver is significantly larger than the distance between it and an eavesdropper. Moreover, the PLS strategy cannot be implemented if the legitimate receiver is located very far away from the UAV transmitter. Although the UAV transmitter can fly close to the legitimate receiver to obtain a higher rate for achieving PLS, the motion energy consumption of the UAV will be undoubtedly increased. *Second*, the UAV transmitter usually needs the channel state information (CSI) [11] of the eavesdropper for realizing the effective power control or trajectory planning. However, there may be some potential unknown eavesdroppers on the ground so that the CSI of them cannot be detected.

Collaborative beamforming (CB) is a feasible method to realize PLS in UAV communications. The UAVs in a network can perform a virtual antenna array (VAA) and use CB to communicate with the legitimate receivers directly, which improves the transmission rate and reduces the risk of information eavesdropping. However, a UAV-based VAA has certain disadvantages, i.e., the beam pattern is damaged

by the randomly distributed UAV elements, which may reduce the performance of the gain. To overcome these shortcomings, the UAV elements can fly to better positions for optimizing the beam pattern. However, this will cause an extra motion energy consumptions of UAVs, such that reducing the network lifetime. Moreover, the excitation current weight of each UAV element is another critical factor that affects the beam pattern as well as the transmission rate. Thus, how to achieve the optimal positions and excitation current weights of the UAV elements in the VAA for achieving better secure communication performance while saving motion energy consumptions by using CB is of great significance.

Different from the previous works that only consider the existence of the detected known eavesdroppers, or aim to optimize secure performance and energy consumptions of UAVs separately, we propose a multi-objective optimization approach that simultaneously optimizes the secure performance under the existence of the known and unknown eavesdroppers and energy consumptions of UAVs.

The main contributions of this paper are summarized as follows:

- We consider a typical secure communication scenario of the UAV networks, i.e., the UAVs perform a VAA to communicate with multi-BSs by using CB. Then, we formulate a secure communication multi-objective optimization problem (MOP) of UAV networks to jointly maximize the total secrecy rate, minimize the total maximum sidelobe levels (SLLs) of UAV-enabled VAA and minimize the total motion energy consumptions of UAVs. Moreover, the formulated problem is proven as NP-hard.
- We analyze the characteristics of the formulated MOP and propose an improved multi-objective dragonfly algorithm with chaotic solution initialization and hybrid solution update operators (IMODACH) to solve the formulated problem. IMODACH uses the chaos theory to enhance the performance of the initial solutions and introduces the hybrid solution update operation to deal with the complex solution space which contains continuous and discrete solutions, so that making the algorithm more suitable for solving the formulated MOP.
- Simulations are carried out to evaluate the effectiveness and performance of the proposed approach.

The rest of this paper is organized as follows: Section II reviews some key related works. Section III gives the models and preliminaries. Section IV formulates the secure communication MOP of UAV networks. Section V proposes the algorithm. Section VI shows the simulation results and Section VII concludes the overall paper.

II. RELATED WORK

In this work, we aim to achieve joint optimizations of secure communication and energy efficiency of UAV networks by using CB. However, these objectives are usually considered separately in the literature, and we briefly present some key works of them to illustrate the novelty of our work.

Zhang et al. [12] study the UAV-enabled wireless communications and formulate an energy minimization problem by jointly optimizing the UAV trajectory, communication time allocation among the ground nodes and total mission completion time. Cheng et al. [13] propose a novel scheme to guarantee the security of UAV-relayed wireless networks with caching by jointly optimizing the UAV trajectory and time scheduling. Sheng et al. [14] propose an Han-Kobayashi signaling for the UAV-enabled multi-user communications, under which the throughput of each pair of users is improved and the eavesdropper is jammed. Zhang et al. [15] also optimize the trajectory of UAV and the transmit power of legitimate transmitter to maximize the average secrecy rates of the UAV-to-ground and ground-to-UAV transmissions, respectively. However, the existence of location-undetectable eavesdroppers are not considered in the abovementioned works.

Some existing works consider the usage of CB in UAV networks. For example, Garza et al. [16] design a UAV-based three-dimensional (3D) antenna array for optimizing the directivity and SLL of the beam pattern. Mozaffari et al. [17] propose a novel framework to deploy and operate a drone-based linear antenna array (LAA) system to minimize the wireless transmission time and control time that are needed for movement and stabilization of the UAVs. However, none of them considers the security and energy efficiency of the UAV networks.

III. MODELS AND PRELIMINARIES

A. System model

As shown in Fig. 1, we consider a UAV-enabled air-to-ground (A2G) wireless communication system, where a set of rotary-wing UAVs denoted as $\mathcal{U} = \{1, 2, \dots, N_{UAV}\}$ are dispatched to communicate with a set of legitimate BSs denoted as $\mathcal{B} = \{1, 2, \dots, N_{BS}\}$, while a set \mathcal{E} of potential eavesdroppers aim to intercept the communications between them. Moreover, we assume that the locations of ground BSs are fixed and known, and there are two types of eavesdroppers that are the known and unknown eavesdroppers exist in the system simultaneously. Specifically, the known eavesdroppers mean that the locations of eavesdroppers can be detected by a camera equipped on the UAV, while the unknown eavesdroppers represent that the locations of eavesdroppers cannot be detected but they must be in the system.

The UAVs will form a VAA to communicate with a set of remote BSs by using CB, wherein each UAV element of the VAA is with a single omnidirectional antenna. Without loss of generality, a 3D Cartesian coordinate system is used in this work, and the locations of the i th UAV, j th BS, p th known eavesdropper and q th unknown eavesdropper are denoted as (x_i^U, y_i^U, z_i^U) , $(x_j^B, y_j^B, 0)$, $(x_p^{KE}, y_p^{KE}, z_p^{KE})$ and $(x_q^{UE}, y_q^{UE}, z_q^{UE})$, respectively.

1) *Array factor of UAV-enabled VAA*: Fig. 1 shows the sketch map of a VAA consists of UAVs to serve different BSs by using CB. According to the principle of electromagnetic

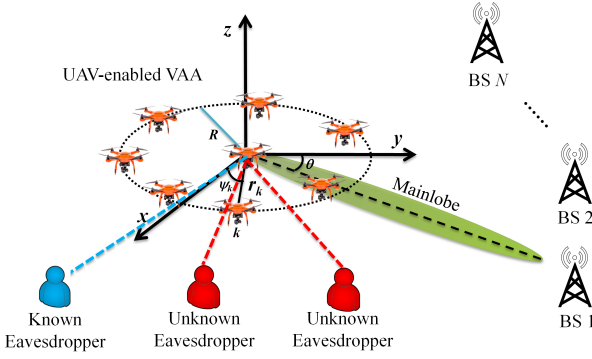


Fig. 1. Sketch map of a UAV-enabled VAA system for CB.

wave superposition, the array factor (AF) can be expressed as follows [16] [18]:

$$AF(\theta, \phi) = \sum_{i=1}^{N_{UAV}} I_i e^{j[k_c(x_i^U \sin \theta \cos \phi + y_i^U \sin \theta \sin \phi + z_i^U \cos \theta)]}, \quad (1)$$

where $\theta \in [0, \pi]$ and $\phi \in [-\pi, \pi]$ are the elevation and azimuth angles, respectively. Moreover, I_i is the excitation current weight of the i th UAV, $k_c = 2\pi/\lambda$ is the phase constant, and λ is the wavelength. As can be seen, AF is directly affected by the locations and excitation current weights of the UAVs.

2) *A2G transmission based on UAV-enabled VAA*: For the A2G transmission, we use the LoS propagation model since the effect of multi-path is significantly mitigated due to the high altitude of UAVs and the usage of CB, and this has been demonstrated by the recent measurement results [17]. Thus, the transmission rate from the UAV-enabled VAA to a receiver in a far-field region is as follows [19]:

$$R_{rec} = B \log_2 \left(1 + \frac{P_{CB_t} K_{rec} G_{rec} d_{rec}^{-\alpha}}{\sigma^2} \right), \quad (2)$$

where B is the transmission bandwidth, P_{CB_t} is the total transmit power of the VAA, K_{rec} is the constant path loss coefficient between the VAA and the receiver, d_{rec} is the distance between the origin of the VAA and the receiver, and σ^2 is the noise power. Moreover, G_{rec} is the gain of the VAA towards the location of the receiver, which is expressed as follows [20]:

$$G_{rec}(\mathbf{x}_j^U, \mathbf{y}_j^U, \mathbf{z}_j^U) = \frac{4\pi |AF(\theta_{rec}, \phi_{rec})|^2 w(\theta_{rec}, \phi_{rec})^2}{\int_0^{2\pi} \int_0^\pi |AF(\theta, \phi)|^2 w(\theta, \phi)^2 \sin \theta d\theta d\phi} \eta, \quad (3)$$

where $(\mathbf{x}_j^U, \mathbf{y}_j^U, \mathbf{z}_j^U) = \{[x_{i,j}^U]_{N_{UAV} \times 1}, [y_{i,j}^U]_{N_{UAV} \times 1}, [z_{i,j}^U]_{N_{UAV} \times 1}\}$ ($i \in \mathcal{U}$) denotes the 3D coordinates of UAVs while communicating with the BS j , and $(\theta_{rec}, \phi_{rec})$ represents the direction towards the receiver. Moreover, $w(\theta, \phi)$ is the magnitude of the far-field beam pattern of each UAV element, $\eta \in [0, 1]$ is the antenna array efficiency [21].

Remark 1. Note that the receiver in this paper can be a BS j ($j \in \mathcal{B}$) or a known eavesdropper KE , and the corresponding

notations above can be expressed as R_{BS_j} , R_{KE} , K_{BS_j} , K_{KE} , d_{BS_j} , d_{KE} , G_{BS_j} and G_{KE} , respectively. \square

B. Energy consumption model of UAV

As derived in [12], the total energy consumption of a UAV includes two main components. The first one is the energy consumptions that related to the communications, i.e., radiation, signal processing and other circuitry. The other one is the energy consumption of propulsion, which ensures the UAV remains hovering and moving. In general, the communication-related energy consumption can be ignored since it is much smaller than propulsion energy, e.g., a few watts (w) versus hundreds of w [12]. Thus, for a rotary-wing UAV with a speed of v , the propulsion power consumption when it flies in a two-dimensional (2D) horizontal plane can be modeled as follows [12]:

$$P(v) = P_B \left(1 + \frac{3v^2}{v_{tip}^2} \right) + P_I \left(\sqrt{1 + \frac{v^4}{4v_0^4}} - \frac{v^2}{2v_0^2} \right)^{1/2} + \frac{1}{2} d_0 \rho s A v^3, \quad (4)$$

where P_B and P_I are the two constants that represent the blade profile power and induced power in hovering status, respectively. v_{tip} is the tip speed of the rotor blade, v_0 is the mean rotor induced velocity in hovering, d_0 and s are the fuselage drag ratio and rotor solidity, respectively, and ρ and A are known as the air density and rotor disc area, respectively.

Remark 2. Note that we ignore the additional/less energy consumption caused by the acceleration/deceleration of the horizontal flight of UAVs since it only takes a small portion of the total operation time of UAV maneuvering duration, as mentioned in [12]. \square

Moreover, by considering the arbitrary 3D UAV trajectory with UAV climbing and descending over time, the energy consumption with the heuristic closed-form approximation is expressed as follows [2]:

$$E(T) \approx \int_0^T P(v(t)) dt + \frac{1}{2} m_{UAV} (v(T)^2 - v(0)^2) + m_{UAV} g(h(T) - h(0)), \quad (5)$$

where $v(t)$ is the instantaneous UAV speed of time t , T represents the end time of the flight, m_{UAV} is the aircraft mass of a UAV, and g is the gravitational acceleration.

Lemma 1. By using the energy consumption models shown in Eqs. (4) and (5), the motion energy consumption of a UAV to fly per unit distance in the vertical direction is more than that in the horizontal direction.

Proof. Eq. (5) has more items than Eq. (4), which causes extra energy consumption. More intuitively, the energy consumption per second of a UAV during the horizontal (E_{hor}) and vertical (E_{ver}) flight at different speeds are shown in Fig. 2. As can be seen, $E_{ver} > E_{hor}$ at different speeds. \blacksquare

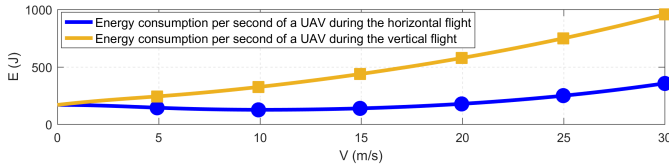


Fig. 2. Energy consumptions of UAV flying in horizontal and vertical directions under different speeds.

C. MOP

Mathematically, an MOP for achieving the minimum value of each objective function can be modeled as follows [22]:

$$\min F = [f_1(x), f_2(x), \dots, f_k(x)], \quad (6)$$

where $f_i(x)$ is the i th objective function, x is the vector of the optimization variables and k is the total number of objective functions.

Different from the single-objective optimization problem, the MOP aims to obtain a non-dominated set of solutions instead of a single optimal solution. In the MOP, the optimal solutions are defined as the Pareto optimal solutions, and the solutions that dominate others but not themselves are defined as the Pareto optimal or non-dominated solutions. Moreover, the set of all the Pareto optimal solutions is defined as the Pareto set (PS) and the set of all the Pareto optimal objective functions is regarded as the Pareto front (PF) [22].

IV. PROBLEM FORMULATION

We consider a square monitor area denoted as A_m . N_{UAV} UAVs are randomly distributed in this area for sensing, data collection or other tasks, and these UAVs can fly to any locations of A_m . Moreover, there are several remote legitimate BSs located far away from A_m , which means that these UAVs cannot reach the BSs for data transmission due to the energy limitation. At a certain time, when the collected data of a UAV, e.g., video or image, reach the upper limit of the catch, or a UAV generates some emergency data that needs to be upload to the BSs immediately, this UAV needs to seek help from other UAVs to form a VAA for CB.

However, due to the existence of eavesdroppers, the secure performance cannot be ignored. Thus, it is necessary to improve the performance of UAV-enabled VAA for achieving a better transmission rate so that the eavesdroppers cannot obtain the sufficient rate. This can be actually achieved by obtaining a better beam pattern of the UAV-enabled VAA, which means that the UAVs can move to better locations and use the optimal excitation current weights to generate a better beam pattern, i.e., with higher directivity, to enhance and reduce the transmission rates from the VAA to the BSs and the known eavesdroppers, respectively. However, the motion energy consumptions of UAVs will be undoubtedly increased, which reduces the lifetime of the UAV networks. Moreover, there are unknown eavesdroppers in the networks, which is also the risk for the data transmissions. Thus, these conditions

should be comprehensively considered since there are trade-offs between them.

In addition, without loss of generality, we assume that the UAVs need to transmit the collected data to all the BSs. However, the mainlobe of the UAV-enabled VAA can point to only one BS at each time, which means that the UAV elements of the VAA need to be re-located after each transmission. Thus, the order of communicating with each BS should be also considered since this will affect the motion energy consumptions of the UAVs.

Accordingly, the optimization objectives are detailed as follows.

Optimization objective 1: The transmission rate from the UAV-enabled VAA to each BS should be maximized. However, due to the existence of the eavesdroppers, the secure performance cannot be ignored. As mentioned in section III-A, the location of the known eavesdropper can be detected, and thus we define the secrecy rate from the UAV-enabled VAA to the j th BS as follows:

$$\begin{aligned} R_{sec_j}^{(U2B)} &= R_{BS_j} - R_{KE} \\ &= B \log_2 \left(1 + \frac{P_{CB_t} K_{BS_j} G_{BS_j} d_{BS_j}^{-\alpha}}{\sigma^2} \right) - \\ &\quad B \log_2 \left(1 + \frac{P_{CB_t} K_{KE} G_{KE} d_{KE}^{-\alpha}}{\sigma^2} \right). \end{aligned} \quad (7)$$

In this paper, the first objective is to maximize the total secrecy rates from the UAV-enabled VAA to all the BSs, and this can be achieved by optimizing the locations and excitation current weights of the UAV elements of VAA and the order of communicating with different BSs. Thus, the first objective function can be designed as follows:

$$f_1(\mathbb{X}^{\mathcal{B} \times \mathcal{U}}, \mathbb{Y}^{\mathcal{B} \times \mathcal{U}}, \mathbb{Z}^{\mathcal{B} \times \mathcal{U}}, \mathbb{I}^{\mathcal{B} \times \mathcal{U}}, \mathbb{Q}^{\mathcal{B} \times 1}) = \sum_{j=1}^{N_{BS}} R_{sec_j}^{(U2B)}, \quad (8)$$

where $(\mathbb{X}^{\mathcal{B} \times \mathcal{U}}, \mathbb{Y}^{\mathcal{B} \times \mathcal{U}}, \mathbb{Z}^{\mathcal{B} \times \mathcal{U}}, \mathbb{I}^{\mathcal{B} \times \mathcal{U}}, \mathbb{Q}^{\mathcal{B} \times 1})$ is the solution to the objective function and it can be expressed in Eq. (9). Specifically, $\mathbb{X}^{\mathcal{B} \times \mathcal{U}}$, $\mathbb{Y}^{\mathcal{B} \times \mathcal{U}}$, $\mathbb{Z}^{\mathcal{B} \times \mathcal{U}}$ and $\mathbb{I}^{\mathcal{B} \times \mathcal{U}}$ denote the 3D locations and excitation current weights of UAVs for serving different BSs, and $\mathbb{Q}^{\mathcal{B} \times 1}$ means the order that the UAV-enabled VAA to communicate with different BSs, respectively. $\mathbb{Q}^{\mathcal{B} \times 1}$ will be introduced in details as follows.

Optimization objective 2: The unknown eavesdroppers cannot be detected by the UAVs. However, they exist in the network, which can be regarded as the potential threats that damage the secure performance. Since the locations of the unknown eavesdroppers cannot be determined by the UAV-enabled VAA, we aim to protect the information security by reducing the maximum SLL of the beam pattern.

Thus, the second objective is to reduce the total maximum SLLs of the UAV-enabled VAA for the transmissions to different BSs, and it can be designed as follows:

$$\begin{aligned} f_2(\mathbb{X}^{\mathcal{B} \times \mathcal{U}}, \mathbb{Y}^{\mathcal{B} \times \mathcal{U}}, \mathbb{Z}^{\mathcal{B} \times \mathcal{U}}, \mathbb{I}^{\mathcal{B} \times \mathcal{U}}, \mathbb{Q}^{\mathcal{B} \times 1}) \\ = \sum_{j=1}^{N_{BS}} \frac{\max |AF(\theta_{SL_j}, \phi_{SL_j})|}{AF(\theta_{ML_j}, \phi_{ML_j})}, \end{aligned} \quad (10)$$

$$X = [\mathbb{X}^{\mathcal{B} \times \mathcal{U}}, \mathbb{Y}^{\mathcal{B} \times \mathcal{U}}, \mathbb{Z}^{\mathcal{B} \times \mathcal{U}}, \mathbb{I}^{\mathcal{B} \times \mathcal{U}}, \mathbb{Q}^{\mathcal{B} \times 1}] = \begin{bmatrix} x_{1,1}^U & \dots & x_{1,N_{UAV}}^U, & y_{1,1}^U & \dots & y_{1,N_{UAV}}^U, & z_{1,1}^U & \dots & z_{1,N_{UAV}}^U, & I_{1,1} & \dots & I_{1,N_{UAV}}, & Q_1 \\ x_{2,1}^U & \dots & x_{2,N_{UAV}}^U, & y_{2,1}^U & \dots & y_{2,N_{UAV}}^U, & z_{2,1}^U & \dots & z_{2,N_{UAV}}^U, & I_{2,1} & \dots & I_{2,N_{UAV}}, & Q_2 \\ \vdots & & & & & & & & & & & & \vdots \\ x_{N_{BS},1}^U & \dots & x_{N_{BS},N_{UAV}}^U, & y_{N_{BS},1}^U & \dots & y_{N_{BS},N_{UAV}}^U, & z_{N_{BS},1}^U & \dots & z_{N_{BS},N_{UAV}}^U, & I_{N_{BS},1} & \dots & I_{N_{BS},N_{UAV}}, & Q_{N_{BS}} \end{bmatrix}. \quad (9)$$

where $(\theta_{SL_j}, \phi_{SL_j})$ and $(\theta_{ML_j}, \phi_{ML_j})$ are the directions of the maximum SLL and mainlobe when the UAV-enabled VAA communicates with BS j , respectively.

Remark 3. It can be seen from Eqs. (1), (2) and (3) that the transmission rate is nonlinear but positively proportional to the AF. Thus, the beam pattern of the UAV-enabled VAA affects the transmission rate directly. In other words, if the maximum SLL of the VAA is suppressed, the received transmission rates of the unknown eavesdroppers are reduced correspondingly. \square

Optimization objective 3: To achieve the previous two objectives, the UAVs need to fly to better locations and perform different VAAs for communicating with different BSs. However, these processes will cause extra motion energy consumptions. To reduce the total motion energy consumptions of the UAVs for performing the VAAs, the third objective function can be designed as follows:

$$f_3(\mathbb{X}^{\mathcal{B} \times \mathcal{U}}, \mathbb{Y}^{\mathcal{B} \times \mathcal{U}}, \mathbb{Z}^{\mathcal{B} \times \mathcal{U}}, \mathbb{Q}^{\mathcal{B} \times 1}) = \sum_{j=1}^{N_{BS}} \sum_{i=1}^{N_{UAV}} E_{i,j}, \quad (11)$$

where $E_{i,j}$ is the total motion energy consumptions of the i th UAV for communicating with the j th BS, and $E_{i,j}(t_{i,j}) = P_{h_{i,j}}(v_{MD_h})t_{h_{i,j}} + P_{v_{i,j}^c}(v_{MD_v^c})t_{v_{i,j}^c} + P_{v_{i,j}^d}(v_{MD_v^d})t_{v_{i,j}^d}$. $P_{h_{i,j}}$, $P_{v_{i,j}^c}$ and $P_{v_{i,j}^d}$ are the horizontal, climb and descend flight powers of the i th UAV for communicating with the j th BS, respectively, $t_{h_{i,j}} = \frac{D_{(i,j)_h}}{v_{MD_h}}$, $t_{v_{i,j}^c} = \frac{D_{(i,j)_v^c}}{v_{MD_v^c}}$ and $t_{v_{i,j}^d} = \frac{D_{(i,j)_v^d}}{v_{MD_v^d}}$ are the corresponding time of the horizontal, climb and descend flights, wherein $D_{(i,j)_h}$, $D_{(i,j)_v^c}$ and $D_{(i,j)_v^d}$ are the corresponding horizontal, climb and descend flights distance that can be determined by $[\mathbb{X}^{\mathcal{B} \times \mathcal{U}}, \mathbb{Y}^{\mathcal{B} \times \mathcal{U}}, \mathbb{Z}^{\mathcal{B} \times \mathcal{U}}, \mathbb{Q}^{\mathcal{B} \times 1}]$. Moreover, v_{MD_h} , $v_{MD_v^c}$ and $v_{MD_v^d}$ are the corresponding maximum-distance (MD) speed of the horizontal, climb and descend flights, respectively.

Remark 4. The MD speed is the optimal UAV speed that maximizes the total flying distance with a unit energy E_u [2]. Thus, we assume that each UAV flies with v_{MD_h} , $v_{MD_v^c}$ and $v_{MD_v^d}$ in different directions in this paper. \square

Accordingly, the secure communication MOP based on UAV-enabled VAA can be formulated as follows:

$$\min_X F = \{-f_1, f_2, f_3\} \quad (12a)$$

$$\text{s.t. } C1 : 0 \leqslant I_{i,j} \leqslant 1, \forall i \in \mathcal{B}, \forall j \in \mathcal{U} \quad (12b)$$

$$C2 : L_{min} \leqslant x_{i,j}^U \leqslant L_{max}, \forall i \in \mathcal{B}, \forall j \in \mathcal{U} \quad (12c)$$

$$C3 : L_{min} \leqslant y_{i,j}^U \leqslant L_{max}, \forall i \in \mathcal{B}, \forall j \in \mathcal{U} \quad (12d)$$

$$C4 : H_{min} \leqslant z_{i,j}^U \leqslant H_{max}, \forall i \in \mathcal{B}, \forall j \in \mathcal{U} \quad (12e)$$

$$C5 : \mathbb{Q}^{\mathcal{B} \times 1} \in \mathcal{Q} \quad (12f)$$

$$C6 : \theta_{SL} \in [-\pi, \theta_{FN1}) \cup (\theta_{FN2}, \pi] \quad (12g)$$

$$C7 : \phi_{SL} \in [-\pi, \phi_{FN1}) \cup (\phi_{FN2}, \pi] \quad (12h)$$

$$C8 : D_{(i_1, i_2)} \geq D_{min}, \forall i_1, i_2 \in \mathcal{U} \quad (12i)$$

where L_{min} and L_{max} are the minimum and maximum ranges of the area that the UAVs can move in the horizontal plane, and H_{min} and H_{max} are the minimum and maximum altitudes that the UAV can fly in the vertical directions, respectively. Moreover, \mathcal{Q} is the set of orders that the UAV-enabled VAA communicates with N_{BS} different BSs, which has $N_{BS}!$ possible permutations. Specifically, $\mathcal{Q} = \{\mathbb{Q}_1^{\mathcal{B} \times 1}, \mathbb{Q}_2^{\mathcal{B} \times 1}, \dots, \mathbb{Q}_{N_{BS}}^{\mathcal{B} \times 1}\}$, wherein an element $\mathbb{Q}_i^{\mathcal{B} \times 1} = \{Q_1, Q_2, \dots, Q_{N_{BS}} | j \in \mathcal{B}, Q_j \in \mathcal{B}\}$. For example, $\mathbb{Q}^{\mathcal{B} \times 1} = \{2, 1, \dots, 10\}$ represents that the VAA will communicate with the these BSs according to the order of BS 2, BS 1, ..., BS 10. In addition, θ_{FN1} , θ_{FN2} , ϕ_{FN1} and ϕ_{FN2} are the first nulls in $[-\pi, \theta_{ML}]$, $(\theta_{ML}, \pi]$, $[0, \phi_{ML}]$ and $(\phi_{ML}, \pi]$, respectively, and they can determine the first null beamwidth of the beam pattern. Furthermore, the constraint in (12i) indicates that the minimum separation distance between two adjacent UAVs must be greater than D_{min} to avoid collision.

Remark 5. For the antenna array beam pattern synthesis, some objectives are trade-offs. For example, if the sidelobe is reduced, more energy will be contained in the mainlobe of the transmitted signal, which may widen the mainlobe beamwidth, causing a low directivity as well as the gain so that reducing the transmission rate. Moreover, the total motion energy consumptions of the UAVs will be increased for achieving better communication performance. Thus, these three optimization objectives are trade-offs. \square

Remark 6. To reach the desired positions, each UAV will first fly along the horizontal direction, then in the vertical direction, which is a common flight method in practice [12]. \square

Lemma 2. The formulated MOP shown in Eq. (12) is NP-hard.

Proof. For ease of analysis and without loss of generality, we only consider the third optimization objective and simplify the original formulated MOP by using fixed locations and excitation current weights of the UAV-enabled VAA. Thus, f_3 and the corresponding constraints can be reduced as follows:

$$\min_{X(\mathbb{Q}^{\mathcal{B} \times 1})} f = \sum_{j=1}^{N_{BS}-1} E_{Q_j, Q_{j+1}} \quad (13a)$$

$$\text{s.t. } \mathbb{Q}^{\mathcal{B} \times 1} \in \mathcal{Q} \quad (13b)$$

where $E_{Q_j, Q_{j+1}}$ denotes the motion energy consumptions of the UAVs from communicating with the Q_j th BS to that of the Q_{j+1} th BS.

The reduced optimization problem (13) is actually a traveling salesman problem (TSP) [19] [23], which is known to be NP-hard. Moreover, the sidelobe reduction optimization problem shown in f_2 has been demonstrated as NP-hard [18] [24]. Since both f_2 and f_3 are NP-hard, then the original formulated secure communication MOP of UAV networks is NP-hard. ■

V. ALGORITHM

In this section, an IMODACH with several improved factors are proposed to solve the formulated MOP.

A. Motivation

Evolutionary as well as swarm intelligence algorithms have the potential to address the NP-hard problems since they are the population-based heuristic search approaches that do not need the gradient information. Among these algorithms, the dragonfly algorithm (DA) is inspired by the static and dynamic swarming behaviors of dragonflies in nature, and it has been demonstrated to be superior to some other algorithms [25]. Thus, we aim to use multi-objective DA (MODA), which is the multi-objective version of conventional DA to solve the formulated secure communication MOP of UAV networks. However, this algorithm may face the following challenges when solving the MOP shown in Eq. (12):

- The formulated MOP in Eq. (12) contains both continuous solution dimensions ($\mathbb{X}^{\mathcal{B} \times \mathcal{U}}, \mathbb{Y}^{\mathcal{B} \times \mathcal{U}}, \mathbb{Z}^{\mathcal{B} \times \mathcal{U}}, \mathbb{I}^{\mathcal{B} \times \mathcal{U}}$) and discrete solution dimensions ($\mathbb{Q}^{\mathcal{B} \times 1}$), which means that it is a hybrid MOP with mixed solution variables. Thus, solving this problem becomes a challenging task for the evolutionary computation algorithms [26].
- In Eq. (12), the positions of UAVs ($\mathbb{X}^{\mathcal{B} \times \mathcal{U}}, \mathbb{Y}^{\mathcal{B} \times \mathcal{U}}, \mathbb{Z}^{\mathcal{B} \times \mathcal{U}}$), the excitation current weights of UAVs ($\mathbb{I}^{\mathcal{B} \times \mathcal{U}}$) and the order of communicating with different BSs ($\mathbb{Q}^{\mathcal{B} \times 1}$) are optimized. Thus, we must optimize $(4 \times (N_{UAV} \times N_{BS}) + N_{BS})$ solution dimensions. Moreover, the number of solution dimensions increases in proportion to both N_{UAV} and N_{BS} , which means that the formulated MOP will become a large-scale optimization problem. For example, assume that the numbers of UAVs and BSs are 20 and 10, respectively, then the number of solution dimension is 810.
- In the formulated MOP, different solution dimensions represent different physical meanings, which means that not all the dimensions are with the same upper and lower bounds. However, the conventional MODA usually update each dimension of solution by using the same method and the identical algorithmic logic results in a lack of specificity for the solution dimensions of a different nature, causing the algorithm to consume unnecessary resources in a redundant solution space.

Thus, the conventional MODA cannot solve the formulated secure communication MOP of UAV-enabled VAA directly and completely, which motivates us to propose the IMODACH.

B. Conventional MODA

In DA, a solution to the optimization problem is represented by a dragonfly, and the algorithm simulates the behaviors of dragonflies according to the mathematical models that are separation S , alignment A , cohesion C , attracted towards food sources *Food*, distracted outward enemies *Enemy* and Lévy flight, respectively [27]. These models above are considered to form a step vector ΔX , and the solution update method of DA can be defined as follows [27]:

$$X_{t+1} = X_t + \Delta X_{t+1}, \quad (14)$$

where X_t denotes the solution in the t th iteration of DA.

To solve MOP, MODA utilizes Pareto optimal dominance for the comparisons between different solutions. Moreover, MODA exploits an archive to maintain the Pareto optimal solutions during the iterative process, and it introduces the hyper-sphere [27] to cover all the solutions of the PS and determines the probability of being abandoned of each solution according to the distribution density of the solution. The details of MODA can be found in [27].

C. IMODACH

In this section, an IMODACH is proposed to solve the formulated secure communication MOP of UAV networks. IMODACH is extended and enhanced from the conventional MODA by using two improved factors that are the chaotic solution initialization and hybrid solution update operators, such that defusing the challenges presented in Section V-A. The general framework of IMODACH is shown in Algorithm 1 and the details are presented as follows.

1) *Chaotic solution initialization operator*: The initial populations in conventional MODA are often generated randomly, which may reduce the population diversity, such that leading to certain blindness of searching directions. Moreover, the formulated MOP shown in (12) has a huge solution space, causing the algorithm may be easy to fall into the local optima, especially when the performance of the initial solutions is not with high quality. Thus, it is necessary to improve the performance of initial solutions.

The chaotic search is a random movement method and it has the natural features of ergodicity, randomicity and irregularity. The main idea of chaos method is to transform the parameters/variables from the solution space to the chaotic domain, which can make the initial solutions to have a better distribution. In this paper, the Guess/mouse map is used since it achieves the best performance of initial solutions in the tests, and this map can be described as follows:

$$\tilde{h}_{k+1} = \begin{cases} 1, & \tilde{h}_k = 0, \\ \frac{1}{mod(\tilde{h}_k, 1)}, & otherwise, \end{cases} \quad (15)$$

where k is the index of the chaotic sequence, and \tilde{h}_k is the k th number of the Guess/mouse sequence. Moreover, mod is

Algorithm 1: IMODACH

```

1 Define the parameters: population size  $N_{pop}$ ,
   maximum iteration  $t_{max}$ , archive set  $Archive$  and
   fitness function, etc. ;
2 for  $i = 1$  to  $N_{pop}$  do
3   Initialize the  $i$ th solution of the population by
      using Eq. (16); //Chaotic initialization
4 end
5 for  $t = 1$  to  $t_{max}$  do
6   Calculate the objective function values of all
      dragonflies and find the non-dominated solutions;
7   Update  $Archive$  with respect to the obtained
      non-dominated solutions;
8   Update the related parameters of MODA;
9   for  $i = 1$  to  $N_{pop}$  do
10    Calculate the step vector  $\Delta X_i$  according to the
        main factors of dragonflies;
11    Update the continuous part  $X_i(\mathbb{X}^{\mathcal{B} \times \mathcal{U}}, \mathbb{Y}^{\mathcal{B} \times \mathcal{U}},$ 
         $\mathbb{Z}^{\mathcal{B} \times \mathcal{U}}, \mathbb{I}^{\mathcal{B} \times \mathcal{U}})$  of  $i$ th dragonfly by using
        Algorithm 2;
12    Update the discrete part  $X_i(\mathbb{Q}^{\mathcal{B} \times 1})$  of  $i$ th
        dragonfly by using Algorithm 3;
13 end
14 end
15 Return  $Archive$ ;

```

the modulo operation. By using this model, each dimension of solution can be initialized as follows:

$$X(d) = LB_d + \hbar_d \times (UB_d - LB_d), \quad (16)$$

where $X(d)$ is the d th dimension of a solution, and LB_d and UB_d are the corresponding upper and lower bounds of the d th dimension of a solution, respectively.

2) *Hybrid solution update operator*: The formulated MOP has both continuous solution space $(\mathbb{X}^{\mathcal{B} \times \mathcal{U}}, \mathbb{Y}^{\mathcal{B} \times \mathcal{U}}, \mathbb{Z}^{\mathcal{B} \times \mathcal{U}}, \mathbb{I}^{\mathcal{B} \times \mathcal{U}})$ and discrete solution space $(\mathbb{Q}^{\mathcal{B} \times 1})$, respectively. Thus, these two parts should be updated separately, as shown in Fig. 3.

For the continuous part, the solutions can be directly updated by using the method of conventional MODA. However, the upper and lower bounds of these solutions are quite different, which means that the searching steps of the algorithm should be set as different values according to different bounds. Moreover, the factors that affect the performance of the optimization results need to be carefully considered.

First, according to the principles of electromagnetism and CB, an antenna array can achieve higher gain when the elements are concentrated with suitable distances [21], e.g., between 0.5λ and λ for avoiding the mutual coupling. Moreover, if the UAVs in the VAA are compactly distributed, less motion energy will be consumed to change the locations of UAVs for serving different BSs. Thus, it is better for the algorithm to centralize the horizontal locations of UAVs $(\mathbb{X}^{\mathcal{B} \times \mathcal{U}}, \mathbb{Y}^{\mathcal{B} \times \mathcal{U}})$ in the earlier iterations.

Inspired by the black hole algorithm (BHA) [28], a black hole method is introduced to achieve the purpose above. Specifically, a center position of the UAV-enabled VAA is selected as a black hole (X_c^{BH}) to guide the update directions of all the UAV elements, and the solution update method for the horizontal locations of UAV elements in the earlier iterations by using the black hole method can be described as follows:

$$X_i(\mathbb{X}^{\mathcal{B} \times \mathcal{U}}, \mathbb{Y}^{\mathcal{B} \times \mathcal{U}}) = X_i(\mathbb{X}^{\mathcal{B} \times \mathcal{U}}, \mathbb{Y}^{\mathcal{B} \times \mathcal{U}}) + \\ rand \times (X_c^{BH} - X_i(\mathbb{X}^{\mathcal{B} \times \mathcal{U}}, \mathbb{Y}^{\mathcal{B} \times \mathcal{U}})), \quad (17)$$

where $X_c^{BH} = [\tilde{E}(\mathbb{X}^{\mathcal{B} \times \mathcal{U}}), \tilde{E}(\mathbb{Y}^{\mathcal{B} \times \mathcal{U}})]$, and $\tilde{E}(\cdot)$ is the averaging operator for calculating the average values of each row of a matrix. $rand$ is a random number generated from 0 to 1.

Second, according to *Lemma 1*, the vertical flight of a UAV consumes more energy than that of the horizontal flight, which means that the update of $\mathbb{Z}^{\mathcal{B} \times \mathcal{U}}$ needs to be more cautious since it may affect the third optimization objective significantly. Thus, the vector $\mathbb{Z}^{1 \times \mathcal{U}}$ which represents the z -axis coordinates of the UAV-enabled VAA when communicates with the first BS obtained by using the update method of conventional MODA is set as a black hole to guide the update of $\mathbb{Z}^{\mathcal{B}' \times \mathcal{U}}$ ($\mathcal{B}' = \{2, 3, \dots, N_{UAV}\}$), and the update method is as follows ($\forall j \in \mathcal{B}'$):

$$X_i(\mathbb{Z}^{j \times \mathcal{U}}) = X_i(\mathbb{Z}^{j \times \mathcal{U}}) + rand \times (X_i(\mathbb{Z}^{1 \times \mathcal{U}}) - X_i(\mathbb{Z}^{j \times \mathcal{U}})). \quad (18)$$

Finally, appropriate excitation current weights $\mathbb{I}^{\mathcal{B} \times \mathcal{U}}$ can change the beam pattern of the UAV-enabled VAA for each communication significantly, which results in a higher transmission rate and lower maximum SLL. In this work, we also use the black hole method to enhance the update performance of the excitation current weights. Specifically, for a solution X_i that needs to be updated, we first select a full solution X_a from the Pareto archive by using the roulette wheel selection, and replace $X_i(\mathbb{X}^{\mathcal{B} \times \mathcal{U}}, \mathbb{Y}^{\mathcal{B} \times \mathcal{U}}, \mathbb{Z}^{\mathcal{B} \times \mathcal{U}})$ by using $X_a(\mathbb{X}^{\mathcal{B} \times \mathcal{U}}, \mathbb{Y}^{\mathcal{B} \times \mathcal{U}}, \mathbb{Z}^{\mathcal{B} \times \mathcal{U}})$. Then, $X_a(\mathbb{I}^{\mathcal{B} \times \mathcal{U}})$ are set as the black hole (X_a^{BH}) to guide the exploitation of $X_i(\mathbb{I}^{\mathcal{B} \times \mathcal{U}})$, and the update method is as follows:

$$X_i(\mathbb{I}^{\mathcal{B} \times \mathcal{U}}) = X_i(\mathbb{I}^{\mathcal{B} \times \mathcal{U}}) + rand \times (X_a^{BH} - X_i(\mathbb{I}^{\mathcal{B} \times \mathcal{U}})). \quad (19)$$

Accordingly, the continuous solution update method is shown in Algorithm 2. Note that ζ is a threshold for regulating and it is calculated as follows:

$$\zeta = \begin{cases} 0.5 - \frac{t}{t_{max}}, & t < \frac{2 \times t_{max}}{5}, \\ \frac{t}{t_{max}} - 0.5, & otherwise. \end{cases} \quad (20)$$

For the discrete part, it cannot be handled by conventional MODA directly since this algorithm is originally proposed for the continuous optimization problems. Thus, a solution update method for the discrete part of the solution is proposed. In this method, we use the *Food* factor W_f and *Inertial* factor W_w of MODA as the thresholds to determine whether a solution should be crossed with *Food* by using the partial mapped crossover (PMX) [29] or mutation [29] operators. The main

Continuous part			Discrete part	
X	Y	Z	II	Q
$\{L_{min}, L_{max}\}$	$\{L_{min}, L_{max}\}$	$\{H_{min}, H_{max}\}$	$\{0, 1\}$	$\{Q\}$

Fig. 3. The solution structure of the formulated MOP.

steps of the discrete solution update method are shown in Algorithm 3.

Algorithm 2: Continuous solution update algorithm

```

1 Calculate the  $\zeta$  by using Eq. (20);
2 Update  $X_i(\mathbb{X}^{\mathcal{B} \times \mathcal{U}}, \mathbb{Y}^{\mathcal{B} \times \mathcal{U}}, \mathbb{Z}^{\mathcal{B} \times \mathcal{U}}, \mathbb{I}^{\mathcal{B} \times \mathcal{U}})$  by using Eq.
   (14);
3 Update  $X_i(\mathbb{Z}^{\mathcal{B} \times \mathcal{U}})$  by using Eq. (18);
4 if  $t < \frac{2 \times t_{max}}{5}$  then
5   if  $rand < \zeta$  then
6     | Update  $X_i(\mathbb{X}^{\mathcal{B} \times \mathcal{U}}, \mathbb{Y}^{\mathcal{B} \times \mathcal{U}})$  by using Eq. (17);
7   end
8 end
9 else
10  if  $rand < \zeta$  then
11    | Select a full solution  $X_a$  from Archive;
12    | Replace  $X_i(\mathbb{X}^{\mathcal{B} \times \mathcal{U}}, \mathbb{Y}^{\mathcal{B} \times \mathcal{U}}, \mathbb{Z}^{\mathcal{B} \times \mathcal{U}})$  by using
      |  $X_a(\mathbb{X}^{\mathcal{B} \times \mathcal{U}}, \mathbb{Y}^{\mathcal{B} \times \mathcal{U}}, \mathbb{Z}^{\mathcal{B} \times \mathcal{U}})$ ;
13    | Update  $X_i(\mathbb{I}^{\mathcal{B} \times \mathcal{U}})$  by using Eq. (19);
14  end
15 end
16 Return  $X_i(\mathbb{X}^{\mathcal{B} \times \mathcal{U}}, \mathbb{Y}^{\mathcal{B} \times \mathcal{U}}, \mathbb{Z}^{\mathcal{B} \times \mathcal{U}}, \mathbb{I}^{\mathcal{B} \times \mathcal{U}})$ ;

```

Algorithm 3: Discrete solution update algorithm

```

1 Define the discrete dimensions of Food  $\mathbb{Q}_{Food}^{\mathcal{B} \times 1}$ , Food
   factor  $W_f$  and Inertial factor  $W_w$ ;
2 if  $W_f * rand > W_w * rand$  then
3   |  $X_i(\mathbb{Q}^{\mathcal{B} \times 1})$  crosses with  $\mathbb{Q}_{Food}^{\mathcal{B} \times 1}$  by using PMX
     operator;
4 end
5 else if  $rand * W_w > 0.1$  then
6   | Update  $X_i(\mathbb{Q}^{\mathcal{B} \times 1})$  by using mutation operator;
7 end
8 Return  $X_i(\mathbb{Q}^{\mathcal{B} \times 1})$ ;

```

D. Complexity of the proposed algorithm

Lemma 3. The complexity of the proposed IMODACH is $\mathcal{O}(k \cdot N_{pop}^2)$.

Proof. The computational complexity of the proposed algorithm is primarily derived by the computations of the objective functions and crowding distance. We assume that the number of optimization objectives and population size are k and N_{pop} , respectively, then the objective function computation has $\mathcal{O}(k \cdot N_{pop})$ computational complexity. Moreover, the cost

part of crowding distance computation is sorting the solutions in each objective function. Specifically, the computational complexity of sorting N_{Arc} solutions in the Pareto archive is $\mathcal{O}(k \cdot N_{Arc} \cdot \log N_{Arc})$. In this paper, we set the size of the Pareto archive to be the same as the population N_{pop} , which means that the computational complexity for the non-dominated sorting is $\mathcal{O}(k \cdot N_{pop}^2)$. Thus, the overall complexity of the proposed IMODACH is $\mathcal{O}(k \cdot N_{pop}^2)$. ■

VI. SIMULATION RESULTS AND ANALYSIS

In this section, we conduct simulations to evaluate the performance of the proposed IMODACH for solving the formulated secure communication MOP of UAV networks by using Matlab.

A. Simulation setups

In our simulation, the monitor region A_m is set as 100 m \times 100 m, and the number of BSs and UAVs are 8 and 16, respectively. Moreover, the carrier frequency (f_c), total transmit power (P_{CB_t}) and path loss coefficient (K_{BS}) are set as 2.4 GHz, $(0.1 \times N_{UAV})$ W and 2, respectively. In addition, the mass (m_{UAV}), collision distance (D_{min}), minimum and maximum altitudes of UAVs (H_{min} and H_{max}) are set as 2 kg, 0.5 m, 100 m and 120 m, respectively. Other key parameters follow the works in [12] and [17].

On the other hand, several comparison methods are introduced to verify the performance of the proposed algorithm. First, the uniform LAA consists of UAV elements is adopted. Note that the LAA means that all the UAV elements are symmetrically excited and located about the origin of the array as done in [17]. Second, we devise an approach named mixed position with optimized excitation current weight (MPOECW) for comparison. In MPOECW, the positions of UAVs for communicating with the first BS is determined by using the conventional MODA and these positions will be unchanged. When the UAV-enabled VAA needs to communicate with the rest BSs, only the excitation current weights of the UAV elements are optimized by using conventional MODA. Finally, the conventional MODA, multi-objective particle swarm optimization (MOPSO), and non-dominated sorting genetic algorithm II (NSGA-II) are introduced to solve the formulated MOP for comparison. Note that the proposed discrete solution update method of the hybrid solution update factor is introduced to these comparison algorithms above so that they are able to deal with the formulated MOP.

In addition, the population size and the maximum iteration are set to 30 and 500, respectively.

B. Optimization results

In this section, the proposed IMODACH and other comparison approaches are used to solve the formulated MOP. Note that the results of MPOECW, MOPSO, NSGA-II, MODA and the proposed IMODACH are selected from the PS with the highest secrecy rate since it is the most important objective in this work. Table I shows the numerical results obtained by different approaches in terms of the total secrecy rates

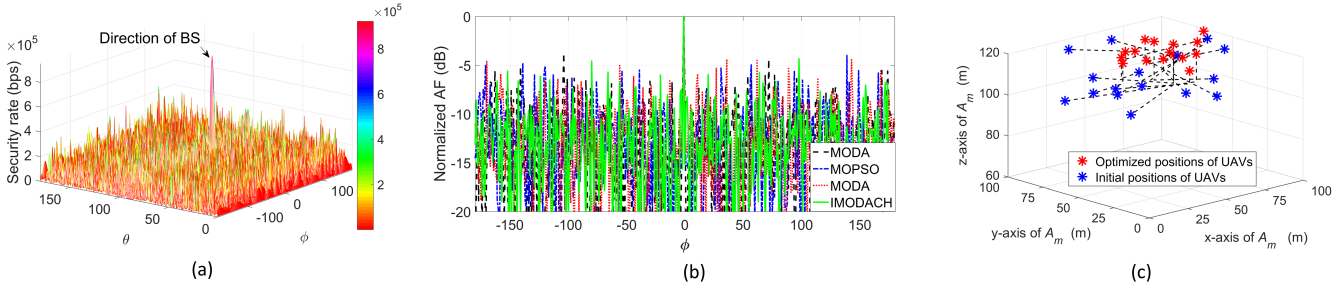


Fig. 4. Optimization results obtained by IMODACH for communicating with the first BS. (a) Secrecy rate distributions between the UAV-enabled VAA and the first BS. (b) Beam patterns. (3) Flight paths of UAVs.

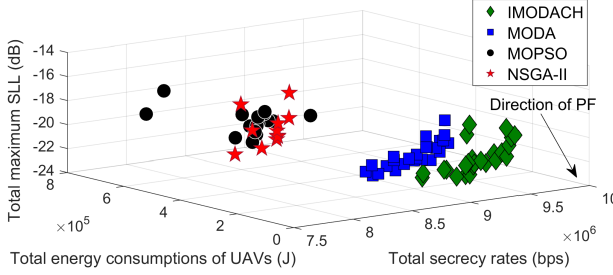


Fig. 5. Solution distributions obtained by different algorithms.

(f_1), total maximum SLLs (f_2) and total energy consumptions of UAVs (f_3). As can be seen, the proposed IMODACH achieves the best performance on the first optimization objectives while it gets the second best results on the second and third optimization objectives. Although the motion energy consumptions of UAVs obtained by IMODACH is a little higher than MPOECW, the difference between these approaches can be ignored since a better secrecy rate can reduce the time for hovering communication with BSs, so that saving the energy consumptions of hovering. Moreover, since the three optimization objectives are trade-offs, it is difficult to achieve the best performance on all the objectives. Thus, IMODACH has the overall best performance among all the approaches. For a more intuitive presentation, the optimization results in terms of the secrecy rate, beam patterns and flight paths of UAVs obtained by the proposed IMODACH for communicating with the first BS is shown in Fig. 4 . Note that due to the page limit, we only present the results for serving one of the eight BSs.

TABLE I
NUMERICAL OPTIMIZATION RESULTS OBTAINED BY DIFFERENT APPROACHES

Method	f_1 (bps)	f_2 (dB)	f_3 (J)
LAA	8.2×10^6	-7.6	2.5×10^5
MPOECW	8.3×10^6	-19.2	6.8×10^4
MOPSO	8.2×10^6	-16.9	2.7×10^5
NSGA-II	8.0×10^6	-14.7	2.3×10^5
MODA	9.1×10^6	-20.3	1.4×10^5
IMODACH	9.7×10^6	-20.0	1.1×10^5

Fig. 5 shows the solution distributions of different multi-

objective optimization algorithms including MOPSO, NSGA-II, conventional MODA and the proposed IMODACH. It can be seen from the figure that the solutions obtained by IMODACH are more closer to the PF and have a more uniform distribution, which means that it has a better performance than other algorithms for solving the formulated MOP. The reason may be that the chaos-based solution initialization method can make the solution to be distributed more uniform, balancing the exploration and exploitation abilities of the algorithm.

VII. CONCLUSION

In this paper, the PLS communications of UAV networks based on CB is investigated. Specifically, we consider a scenario which exists a known eavesdropper and several unknown eavesdroppers, and formulate a secure communication MOP of UAV networks to simultaneously enhance the total secrecy rates, total maximum SLLs and total motion energy consumptions of UAVs. Moreover, the NP-hardness of the problem is proven. The solution to the formulated MOP is hybrid and complex, which contains continuous and discrete parts, respectively. Thus, an IMODACH method is proposed to solve this problem. IMODACH uses the chaos method to enhance the quality of initial solutions and introduces the hybrid solution update method to deal with the hybrid solutions of the formulated MOP, so that improving the performance of the algorithm. Simulations are conducted to evaluate the effectiveness of the proposed algorithm and the results show that IMODACH achieves the overall best performance in terms of the three optimization objectives for communicating with different BSs than some other benchmark methods including LAA, MPOECW, MOPSO, NSGA-II and conventional MODA.

ACKNOWLEDGMENT

This study is supported in part by the National Natural Science Foundation of China (62002133, 61872158, 61806083), in part by the Science and Technology Development Plan Project of Jilin Province (20190701019GH, 20190701002GH), and in part by the CERNET Innovation Project (NGII20190802). Geng Sun is the corresponding author.

REFERENCES

- [1] Z. Ullah, F. Al-Turjman, and L. Mostarda, "Cognition in uav-aided 5g and beyond communications: A survey," *IEEE Transactions on Cognitive Communications and Networking*, 2020.
- [2] Y. Zeng, Q. Wu, and R. Zhang, "Accessing from the sky: A tutorial on uav communications for 5g and beyond," *Proceedings of the IEEE*, vol. 107, no. 12, pp. 2327–2375, 2019.
- [3] X. Zhong, Y. Guo, N. Li, and Y. Chen, "Joint optimization of relay deployment, channel allocation, and relay assignment for uavs-aided d2d networks," *IEEE/ACM Transactions on Networking*, vol. 28, no. 2, pp. 804–817, 2020.
- [4] G. Faraci, C. Grasso, and G. Schembra, "Reinforcement-learning for management of a 5g network slice extension with uavs," in *IEEE INFOCOM 2019-IEEE Conference on Computer Communications Workshops (INFOCOM WKSHPS)*. IEEE, 2019, pp. 732–737.
- [5] M. Mozaffari, W. Saad, M. Bennis, Y.-H. Nam, and M. Debbah, "A tutorial on uavs for wireless networks: Applications, challenges, and open problems," *IEEE Communications Surveys & Tutorials*, vol. 21, no. 3, pp. 2334–2360, 2019.
- [6] B. Li, Z. Fei, and Y. Zhang, "Uav communications for 5g and beyond: Recent advances and future trends," *IEEE Internet of Things Journal*, vol. 6, no. 2, pp. 2241–2263, 2018.
- [7] G. Wu, Y. Miao, Y. Zhang, and A. Barnawi, "Energy efficient for uav-enabled mobile edge computing networks: Intelligent task prediction and offloading," *Computer Communications*, vol. 150, pp. 556–562, 2020.
- [8] D. Xu, Y. Sun, D. W. K. Ng, and R. Schober, "Multiuser miso uav communications in uncertain environments with no-fly zones: Robust trajectory and resource allocation design," *IEEE Transactions on Communications*, vol. 68, no. 5, pp. 3153–3172, 2020.
- [9] L. Shi, S. Xu, H. Liu, and Z. Zhan, "Qos-aware uav coverage path planning in 5g mmwave network," *Computer Networks*, p. 107207, 2020.
- [10] B. Bera, S. Saha, A. K. Das, N. Kumar, P. Lorenz, and M. Alazab, "Blockchain-envisioned secure data delivery and collection scheme for 5g-based iot-enabled internet of drones environment," *IEEE Transactions on Vehicular Technology*, 2020.
- [11] S. Piao, Z. Ba, L. Su, D. Koutsonikolas, S. Li, and K. Ren, "Automating csi measurement with uavs: from problem formulation to energy-optimal solution," in *IEEE INFOCOM 2019-IEEE Conference on Computer Communications*. IEEE, 2019, pp. 2404–2412.
- [12] Y. Zeng, J. Xu, and R. Zhang, "Energy minimization for wireless communication with rotary-wing uav," *IEEE Transactions on Wireless Communications*, vol. 18, no. 4, pp. 2329–2345, 2019.
- [13] F. Cheng, G. Gui, N. Zhao, Y. Chen, J. Tang, and H. Sari, "Uav-relaying-assisted secure transmission with caching," *IEEE Transactions on Communications*, vol. 67, no. 5, pp. 3140–3153, 2019.
- [14] Z. Sheng, H. D. Tuan, A. A. Nasir, T. Q. Duong, and H. V. Poor, "Secure uav-enabled communication using han–kobayashi signaling," *IEEE Transactions on Wireless Communications*, vol. 19, no. 5, pp. 2905–2919, 2020.
- [15] G. Zhang, Q. Wu, M. Cui, and R. Zhang, "Securing uav communications via joint trajectory and power control," *IEEE Transactions on Wireless Communications*, vol. 18, no. 2, pp. 1376–1389, 2019.
- [16] J. Garza, M. A. Panduro, A. Reyna, G. Romero, and C. d. Rio, "Design of uavs-based 3d antenna arrays for a maximum performance in terms of directivity and sll," *International Journal of Antennas and Propagation*, vol. 2016, pp. 1–8, 2016.
- [17] M. Mozaffari, W. Saad, M. Bennis, and M. Debbah, "Communications and control for wireless drone-based antenna array," *IEEE Transactions on Communications*, vol. 67, no. 1, pp. 820–834, 2018.
- [18] G. Sun, Y. Liu, Z. Chen, A. Wang, Y. Zhang, D. Tian, and V. C. Leung, "Energy efficient collaborative beamforming for reducing sidelobe in wireless sensor networks," *IEEE Transactions on Mobile Computing*, 2019.
- [19] Y. Zeng, X. Xu, and R. Zhang, "Trajectory design for completion time minimization in uav-enabled multicasting," *IEEE Transactions on Wireless Communications*, vol. 17, no. 4, pp. 2233–2246, 2018.
- [20] K. Venugopal, M. C. Valenti, and R. W. Heath, "Device-to-device millimeter wave communications: Interference, coverage, rate, and finite topologies," *IEEE Transactions on Wireless Communications*, vol. 15, no. 9, pp. 6175–6188, 2016.
- [21] C. A. Balanis, *Antenna Theory: Analysis and Design*, 3rd ed. Hoboken, NJ: John Wiley, 2005.
- [22] Q. Lin, S. Liu, K.-C. Wong, M. Gong, C. A. C. Coello, J. Chen, and J. Zhang, "A clustering-based evolutionary algorithm for many-objective optimization problems," *IEEE Transactions on Evolutionary Computation*, vol. 23, no. 3, pp. 391–405, 2018.
- [23] A. Ouaarab, B. Ahiod, and X. Yang, "Discrete cuckoo search algorithm for the travelling salesman problem," *Neural Computing and Applications*, vol. 24, no. 7-8, pp. 1659–1669.
- [24] S. Liang, Z. Fang, G. Sun, Y. Liu, G. Qu, S. Jayaprakasam, and Y. Zhang, "A joint optimization approach for distributed collaborative beamforming in mobile wireless sensor networks," *Ad Hoc Networks*, vol. 106, p. 102216, 2020.
- [25] S. Khalilpourazari and S. Khalilpourazary, "Optimization of time, cost and surface roughness in grinding process using a robust multi-objective dragonfly algorithm," *Neural Computing and Applications*, vol. 32, no. 8, pp. 3987–3998, 2020.
- [26] Y. Wang, Z.-Y. Ru, K. Wang, and P.-Q. Huang, "Joint deployment and task scheduling optimization for large-scale mobile users in multi-uav-enabled mobile edge computing," *IEEE Transactions on Cybernetics*, 2019.
- [27] S. Mirjalili, "Dragonfly algorithm: A new meta-heuristic optimization technique for solving single-objective, discrete, and multi-objective problems," *Neural Computing and Applications*, vol. 27, no. 4, pp. 1053–1073, 2016.
- [28] A. Hatamlou, "Black hole: A new heuristic optimization approach for data clustering," *Information sciences*, vol. 222, pp. 175–184, 2013.
- [29] K. Deep and H. Mebrahtu, "Variant of partially mapped crossover for the travelling salesman problems," *International Journal of Combinatorial Optimization Problems and Informatics*, vol. 3, no. 1, p. 24, 2012.